Investigation of Vortex Depth in a Partially-Baffled Tank

William Funkenbusch, Luke Oluoch, Sabrina Westgate, Sean Wilson-Leslie

University of Rochester
SPX Lightnin®

Abstract

Vortex formation is important for the incorporation of gases or light solids into stirred tanks. However, large vortices formed in unbaffled tanks fail to facilitate good mixing. Because of this, partially-baffled tanks, which allow for both mixing and vortex formation, are often used in these applications. In this experiment, vortex formation was studied in a partially-baffled tank with changing parameters of tank size, impeller size, coverage, Fr, and viscosity. Preliminary predictive models were created using significant factors for all of the trials maximum vortex depth, all of the trials average vortex depth, 1 *cP maximum vortex depth,* 100 *cP maximum vortex depth, and* 1000 *cP maximum vortex depth. While these models in their current form do not accurately predict vortex depth, they do predict qualitatively the effect of altering a single system parameter.*

Contents

1 Introduction

1.1 Motivation

In certain applications, such as waste disposal and fermentation, solids must be incorporated into a mixing tank. In these situations, mixing no longer depends only on the homogeneous phase, but also on the interface between the mixing fluid and the solid to be incorporated. Depending on properties of the solid such as density and solubility, the incorporation of the solid might become rate-limiting step in the mixing process. Because of this, traditional baffled tanks may be sub-optimal because the surface of the tank doesn't undergo significant deformation. In an unbaffled tank, formation of a vortex can be easily achieved, but the sufficient mixing of the bulk fluid is sacrificed. To resolve this issue, partially-baffled tanks are used. These tanks are baffled in their lower section and unbaffled in their upper section. Vortex formation occurs in the unbaffled region, allowing solid incorporation, while good mixing of the homogeneous phase is maintained in the baffled section.

When trying to optimize solid incorporation in a partially-baffled tank, vortex depth is an important parameter. As vortex size increases, the area of contact between the solid and fluid increases, thus increasing the rate of incorporation. However, there is a trade-off because larger vortices require larger power inputs and vortices which are too large may interfere with the impeller, cause undesired incorporation of air into the system, or decrease the size of the baffled region significantly. Therefore, if vortex depth could be predicted based on tank and fluid parameters, more efficient incorporation can be achieved without intensive case-by-case testing.

1.2 Theory

1.2.1 Dimensionless Numbers

Research experiments are often not economically viable when run on an industrial scale, yet can obtain results for processes of such size by using Dimensionless numbers. Dimensionless numbers do not rely on the absolute size of a system, and thus are useful for designing processes which can survive scale-up.

For measurements of dimensionless vortex depth (vortex depth per impeller diameter) in geometrically equivalent systems, four dimensionless numbers play an important role: dimensionless impeller diameter (D/T), the Froude number (Fr), Reynolds number (Re), and dimensionless coverage (COV/D).

Dimensionless impeller diameter is the ratio between the impeller diameter and tank diameter. It was hypothesized that larger impellers would create larger vortices and lead to larger power draw from the motor for a given impeller speed. Impeller diameter should thus be the smallest possible while still providing sufficient mixing.

The Froude number is the ratio of the inertial forces of a fluid to the external field, in this case, gravity. It is given by the equation:

$$Fr = \frac{N^2 D}{1.39 \times 10^6} = \frac{u_0}{\sqrt{g_0 l_0}} \tag{1}$$

Where N is the impeller angular velocity, in RPM, D is the impeller diameter, in inches, and the constant is standard gravity expressed in the proper units to make Fr dimensionless. In its most general form, (right hand side) the Froude number is defined as the characteristic flow velocity u_0 over the square root of gravitational force g_0 times characteristic length l_0. The larger the inertial forces in a tank, the greater the outward force moving fluid towards the edge of the tank relative to the restoring force of gravity. Thus, as Fr increases, dimensionless vortex depth was expected to increase for a constant impeller diameter. Froude number was adjusted by varying the impeller speed for each impeller diameter. However, the presence of baffles in this experiment limits the accumulation of fluid momentum inside the tank, thus complicating the interaction between Froude number and vortex depth.

The Reynolds number relates the inertial forces to the viscous forces of a fluid. It is given by the equation:

$$Re = \frac{SG \times N \times D^2 \times 10.754}{\mu} \tag{2}$$

Where SG is the specific gravity of the fluid, μ is the fluid viscosity, N and D are parameters defined above for Fr, and 10.754 is a constant to make the number dimensionless. As the viscosity of a fluid increases, the fluid becomes more resistant to the formation of a vortex because larger vortices shear the fluid more. Thus, as Re decreases, dimensionless vortex depth was expected to decrease. Re naturally changes for different tests as the target Froude number is reached. Fr remains constant for changes in viscosity, while Re does not. Thus, changes in Re show their direct effect in changes in viscosity.

The final dimensionless number used was the dimensionless coverage COV, defined as the ratio between the height of stationary fluid above the center of the impeller to the diameter of the impeller. Coverage can vary between 0 and its value when the fluid reaches the top of the tank. As coverage increases the impeller has to shear more fluid to create a vortex,

resulting in a smaller vortex. However, if coverage is too low the impeller will be unable to shear the fluid further due to loss of contact between the fluid and the blades.

1.2.2 Baffles

Baffles are long vertical protrusions along the tank wall that break up fluid flow and encourage vertical mixing. They are usually employed to help prevent the formation of vortices and facilitate mixing. The ideal sizing of a baffle is to have a thickness of 1/12 that of the tank diameter, and to be spaced about 1/3 of its thickness away from the tank wall [1]. Placing the baffles away from the tank wall prevents dead zones from forming in the corners where a baffle comes flush with the wall. The 1/3 distance also assures that the baffles don't protrude too far into the tank that they would impede mixing or face too great of a mixing force from the moving fluid [1]. For ideal mixing $3-4$ baffles are situated equally around the tank.

1.2.3 Impellers

Two impellers, an A200 and an A310, were attached to the shaft. Both of these are axial type impellers, designed to promote vertical mixing more effectively than radial impellers. This choice encourages thorough mixing and prevents the formation of a dead zone at the bottom of the tank. The A200 (Figure 1, right) has four flat, rectangular fins which, due to a difference in angular velocity, push fluid with much more force towards their edges than towards their centers. This creates a powerful but uneven disruption of water, which is ideal for the unbaffled section of the tank. The A310 (Figure 1, left) has three tapered fins, whose angles of attack become less aggressive away from the center of the impeller. This lower angle counteracts the faster angular velocity at larger radii, generating even flow along the blade. A more aerodynamic shape also reduces the work needed for the impeller to achieve a given rotational speed. The more even flow prevents eddy formation at the base of the tank, so an A310 is ideal for the baffled section of the tank.

1.2.4 Parameters

The parameters that were changed over the course of the experiment were:

- D/T: The ratio between the diameter of the A200 impeller (D) and the diameter of the tank (T). This ratio was varied by changing D.

Figure 1: A310 (left) and A200 (right) impellers

Figure 2: Tachometer in tank setup

- COV/D: The dimensionless coverage, defined as the ratio between the height of fluid above the A200 impeller (COV) and the diameter of the A200 impeller.

- $MixerSpeed$: The speed at which the impellers rotates in RPM.

- μ: The viscosity of the fluid.

2 Experimental

2.1 Mixer Speed

Vortices were expected to be parabolic, as observed by Deshpande et. al. [2]. However, because this experiment was done using a partially-baffled tank as opposed to an unbaffled tank, the exact shape of the vortices was unknown. Each experiment was recorded by a camera giving a side-view of the tank, allowing for examination of vortex stability and shape. From these videos, maximum and average vortex depth, fraction of time a vortex appeared, and any notable characteristics were recorded.

(a)

(b)

Figure 3: (a) the bearing at the center of the 17.5" tank and (b) the original baffles

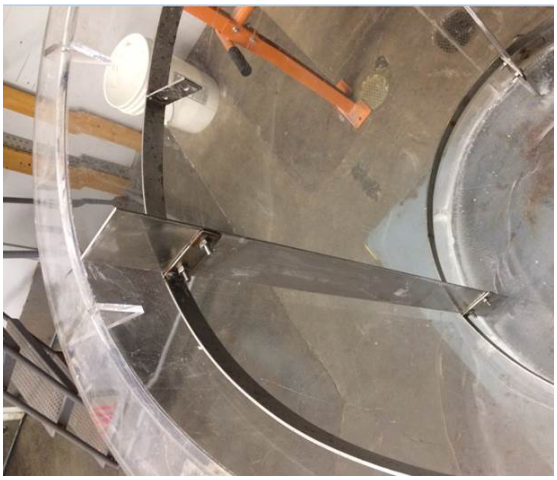

Figure 4: New baffle design, photo from SPX Lightnin

2.2 Tank Setup

For this experiment, two tank sizes were investigated: an 11.5" diameter tank, and a 17.5" diameter tank. The 17.5" diameter tank was already situated in the Gavett Lab is the property of the Chemical Engineering Department, and started with full baffles. SPX provided an 11.5" diameter tank with partial baffles. The speed of the larger tank's impeller was controlled by adjusting the power input, while the smaller tank's impeller speed was controlled by selecting an RPM, allowing for more precise control in the smaller tank. The larger tank contained a plastic bearing which helped to steady the shaft. The bearing has a diameter of 0.55", and a height of 1" (see Figure 3). The smaller tank did not have a bearing, but had a short enough shaft that it did not wobble excessively.

2.3 Tank Deconstruction

In order to use the 17.5" tank already in Gavett, there were a few adjustments made in order to begin testing. The first task was to disassemble the current baffle setup. Four plastic baffles ran the entire height of the tank and attached to the tank with a screw at the top (see Figure 5b). The other two aspects of this deconstruction were removal of the gas sparger ring in the bottom, which was attached to one of the baffles and came out of the tank (see Figure 5c), and the DO probe which measures dissolved oxygen in the tank (see Figure 5d). The original tank setup is shown in Figure 3.

2.4 Tank Baffles

Based upon the ideal ratios of tank diameter to baffle thickness [1], and in agreement with the typical dimensions that SPX uses, baffles 1.5"' thick were placed 0.5"' away from the tank wall. Per the experimental instructions of the project outlined by SPX, the top of the baffles were placed at the same height as the center of the A200 impeller, 10.5"' from the bottom of the tank.

In order to maintain consistency between tanks, the 17.5" tank was fitted with stainless steel baffles. Baffles used in a previous CHE Senior Design project were cut down from their 28" height to 10.5" holes were drilled which allow the baffles to sit 0.5" away from the tank wall. To attach the baffles to the tank, stainless steel ring loops were provided by SPX that fit in the tank as pictured below4. The bottom and top ring loops attach 2" from the bottom of the baffle 2" from the top of the baffle respectively .

2.5 Tank Restoration

To restore the 17.5" tank to its original condition, full baffles must be re-installed. One option for this is to use the old plastic baffles that were originally installed in the tank, seen Figure 3b. The gas sparger ring (see Figure 5c) attaches to one of these baffles. The old plastic baffles can then be bolted onto the tank and Dissolved Oxygen (D. O.) probe can be swiveled back into the tank.

However, a second option for re-installation is available. Using the ring loops provided to us by SPX, Gavett mixing tank would have the ability to hold a variety of baffle heights set at 0.5" from the tank wall. The old baffles, which were flush with the tank wall, often caused dead zones and immature mixing. By separating the baffles from the wall, these dead zones can be eliminated [1]. In this second reconstruction approach, existing stainless steel baffles would be in-

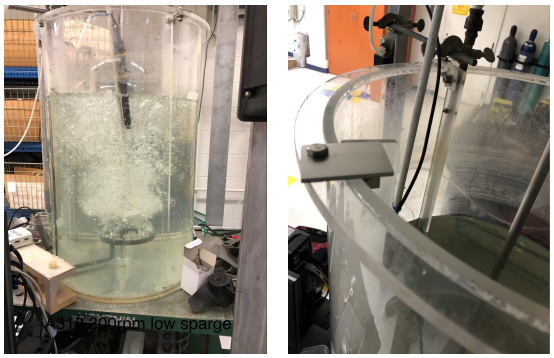

(a) (b)

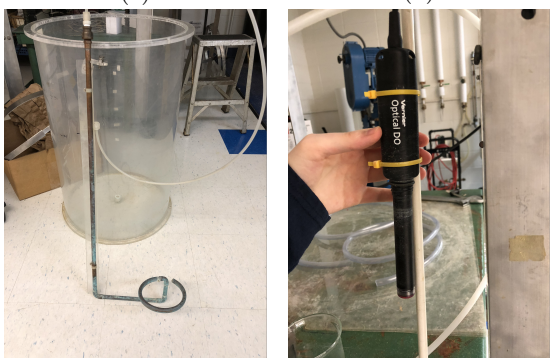

(c) (d)

Figure 5: Old tank setup. (a) the tank while stirring with sparge opened, (b) the old baffles' connection to the tank, (c) the sparge, and (d) the DO probe.

stalled using a ring loop setup 0.5" away from the wall, and would span the height of the tank (28"). The gas sparger ring could then be fastened to the wall apart from the baffles, so as to allow easy removal of the baffles without interfering with the gas sparger. If another set of holes were bored into the baffles, the wall separation could be reduced to only 0.25" away from the wall, or even flush with the wall. This extra set of holes could be plugged with a screw when not in use and would allow Junior Lab students to explore the effect of baffle distance from the wall on mixing. In the same vein, the partial 10.5" baffles would be left with the mixing setup, as to allow Junior Lab students to look at the effect of the baffle heights on fluid mixing. Reconstructing the tank in this fashion would allow future students more flexibility in their mixing experiments.

2.6 P&ID

The P&ID for the 17.5" diameter tank setup is shown in Figure 6. A larger version can be found in Appendix H. All absolute values were scaled down for the 11.5" diameter tank setup. As shown, the diameter of the A310 (lower) impeller and the baffle dimensions were be fixed for each tank diameter. The A200 (upper) impeller was placed such that its center lay at the same height as the top of the baffles. The A200 impeller diameter to tank diameter ratio and coverage to impeller diameter ratio were to be varied. In addition, the impeller speed was be changed to span the range of vortex formation without gas dispersion. Finally, all experiments were be run for fluid viscosities of 1, 100, and 1000 cP.

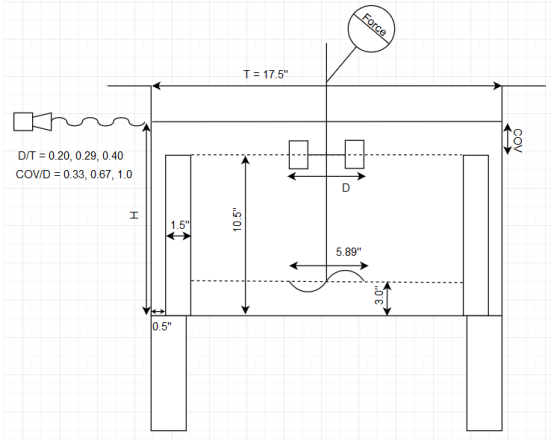

Figure 6: P&ID of 17.5" tank setup

3 Procedure

3.1 Measured Parameters

T (in.)	11.5	17.5	
D/T	0.2	0.29	0.4
COV/D	0.33	0.67	1.0
Fr	Min	Average	Max
μ **(cP)**	1	100	1000

Table 1: Values of the parameters used for the experiment

Impeller	**D** (11.5")	**D** (17.5")
A200	2.30, 3.36, 4.60	3.50, 5.08, 7.00
A310	3.88	5.89

Table 2: Equipment specifications, in inches

Parameter	Label
μ	A
T	B
D/T	C
COV/D	D
Fr	E

Table 3: Letter assignments for each parameter.

3.2 Order of Operations

For each tank diameter, trials were ordered hierarchically by viscosity, then D/T, then COV/D, then mixer speed. For each T, viscosity, D/T, and COV/D, the minimum mixer speed was first found by incrementally increasing the mixer speed and waiting for at least 30 seconds. If no vortex formed in that time, the mixer speed was increased again. The size of each increment was left to visual judgment, and if a vortex appeared suddenly during the increment, the mixer was stopped and the process was repeated with a smaller increment. After reaching steady-state (at least two minutes), a three minute, side-view video of the tank can be recorded and then analyzed . During the trial, vortex depth and stability was qualitatively commented on, as well as any notable features of the particular trial.

Once the minimum mixer speed trial was completed, the maximum mixer speed was found by augmenting gradually the mixer speed until the vortex made regular contact with the impeller. The mixer speed was then decreased until the vortex no longer reached the impeller, and a trial was run using this as the maximum mixer speed. Finally, a third trial was run by decreasing the mixer speed until it was approximately the average of the minimum and maximum mixer speeds.

After these trials were run, the COV/D ratio was then changed and the process was repeated. Once each COV/D was completed, D/T was changed and trials were run for each COV/D and mixer speed. Thus, for each viscosity and tank diameter, a total of 27 trials were run. With three viscosities and two tank diameters, this led to a total of 162 trials.

3.3 Higher Viscosity Fluids (100 cP & 1000 cP)

Higher viscosity fluids were prepared by adding Carbopol 941 to water. For 100 cP, 0.05 wt% was used, and for 1000 cP, 0.10 wt% was used. The tank was first filled with water to the height for a COV/D of 1.0 for the largest impeller. The mixer was run while containing the experimental baffles and Carbopol was slowly added to avoid accumulation of Carbopol around the impeller. The tank was then left stirring for three hours. Next, $3M$ hydrochloric acid was added drop-wise while monitoring the acidity of the solution. The acidity was left to stabilize before each addition of acid. The acid was added until the pH of the solution reached 4.0.

To remove the higher viscosity fluid from the tank, $3M$ sodium hydroxide was added to the tank until the pH of the solution reached 6.0, which decreased its viscosity. The solution was then siphoned into the sink and drained with excess water.

3.4 Coverage

Two tanks were utilized allowing for scaling of data for a range of tank sizes. A 17.5" tank was received from Gavett and baffles. An 11.5" tank was acquired from SPX, along with smaller baffles. The 11.5" tank is approximately 60% the size of the other tank, and all significant distances across the two tanks scale accordingly. Three sizes of A200 impellers are used for each tank. The impeller sizing depends on a ratio between the impeller diameter and tank diameter. The water level in the tank also changes based on a measure of coverage above the top impeller. Coverage is defined as a ratio between the depth of water above an impeller to the impeller diameter, and therefore a fill of 0.33 differs for each A200 diameter used.

4 Results

For the analysis, each parameter was given a single letter label to improve readability. The labels assigned to each parameter are shown in Table 3. All data and fits are tabulated in Appendices B-F.

4.1 Average Vortex Depth

For industrial applications, steady processes with low variances are most desirable. Therefore, average vortex depth serves as an effective quality to measure. For some trials, especially with 1 cP, the vortex was too sporadic for the average depth to be representative of the system, so only a fraction of the trials could be used for this analysis. Pareto analysis on all of the data gives the significant factors shown in Table 4. The model and main effects plots can be found in Appendix B. From this analysis, COV/D and D/T appear to be the most significant individual parameters, with negative correlation between both parameters and average vortex depth.

However, when regressed using just the significant coupled parameter of D/T COV/D, the R^2 value

Parameter	Significance
CD	$p < 0.01$

Table 4: Pareto significant factors for average vortex depth.

equals 0.1120, suggesting a poor fit of the model to the data. This means that the current model is insufficient for predicting the average vortex depth, but the model can still be used qualitatively. For example, for a system which can produce steady vortices and for which D/T is fixed due to resource availability, COV/D should be selected first, adjusting Fr to produce the desired vortex depth. COV/D should be selected to be as small as possible because the required power (proportional to Fr) for a given vortex depth decreases as COV/D decreases. For example, if one desires a vortex of depth Δ with no gas dispersion, COV/D should be selected as $\Delta + \delta$, where δ is the maximum deviation of the vortex from its average value. It is important to note, for this and the remainder of the analysis, that the vortex width, an important and potentially widely variable parameter for solids incorporation, was not analyzed. For better fine-tuning, this parameter needs to be studied as well.

4.2 Maximum Vortex Depth

In certain applications, the primary concern may not be speed of incorporation, but risk management. In these cases, rather than the average, the worst case scenario must be examined. Therefore, analysis was also done on the maximum vortex depth. Maximum vortex depth was calculable for all trials where a vortex appeared, expanding the possible depth of analysis.

First, Pareto analysis was performed on the entire data set. The significant factors are shown in Table 5 and the standardized effects and main effects plots can be found in Appendix C. The analysis showed that the most important factors were again D/T and Fr, with the same overall trends found for the average vortex depth. Regression provided an R^2 value of 0.3391, which, again, suggests poor quantitative fit of the model to the data. However, this fit is notably better than that of the average vortex depth, with a much larger R^2 value and only two uncoupled parameters opposed to five coupled parameters. While the same conclusions can be drawn with the maximum vortex depth as the average vortex depth, the increased simplicity of the model and size of relevant data allow for additional analysis and extrapolation.

Parameter	Significance
E	$p < 0.01$
C	$p < 0.05$

Table 5: Pareto significant factors for maximum vortex depth, all data.

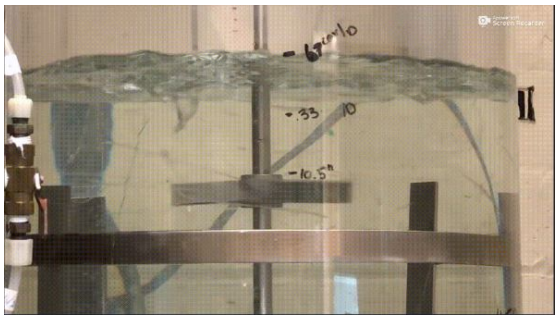

Figure 7: 1 cP trial vortex.

4.3 1 cP Trends

Of particular interest is the vortex depth at a particular fluid viscosity, as in practical applications this is often a constraint on the system rather than a controllable parameter. In the water (1 cP) trials, vortices were sporadic (lasting on the order of seconds), danced around the shaft, and were thin and deep without a defined shape. For an image of a typical vortex in these trials, see Figure 7.

The Pareto significant factors for the water trials are shown in Table 6, and the standardized effects and main effects plots can be found in Appendix D. The most significant effects were tank size and Fr, and it was expected that maximum vortex depth would increase with increasing tank size as well and increasing Fr. The model further corroborates these trends with the F-value for Fr being the highest at 36.83, followed by an F-value of 9.49 for tank size and 4.8 for D/T (see Appendix D). The R^2 value for the predictive model is 0.4767, most likely so low due to the unpredictability and instability of 1 cP liquid material.

Parameter	Significance
E	$p < 0.01$
B	$p < 0.01$
C	$p < 0.05$

Table 6: Pareto significant factors for maximum vortex depth, 1 cP.

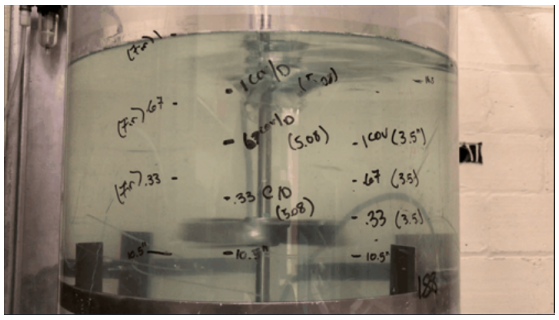

Figure 8: 100 cP trial vortex.

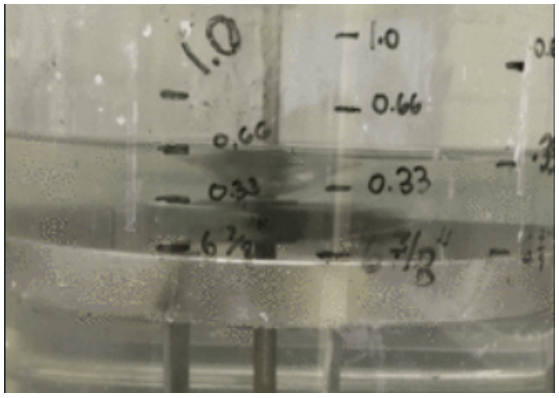

Figure 9: 1000 cP trial vortex.

4.4 100 cP Trends

For the 100 cP and 1000 cP trials, the vortices were much more stable. However, the required Fr to form a vortex was much higher, to the point that the motors were unable to form a vortex for some high COV/D and low D/T. Typical vortices for in these trials, see Figures 8 and 9.

The Pareto significant factors for the 100 cP are shown in Table 7, and the standardized effects and main effects plots can be found in Appendix E. The most significant effects are Fr, D/T, and COV/D. As shown in the main effects plots, as Fr and D/T increase, maximum vortex depth increase, and as COV/D increases, maximum vortex depth decreases. This is in-line with expectations, as is the fact that the F values of the model for Fr is the highest at 57.31, followed by the two way D/T and COV/D interaction. The R^2 value for the 100 cP model is the highest of all the created models at 0.6042. This makes sense with the data because the 1 cP trials had less stable vortices that were hard to characterize, and the 1000 cP trials have missing data because they were unable to form vortices in some conditions.

Parameter	Significance
E	$p < 0.01$
CD	$p < 0.01$
CDE	$p < 0.01$

Table 7: Pareto significant factors for maximum vortex depth, 100 cP.

Parameter	Significance
E	$p < 0.01$

Table 8: Pareto significant factors for maximum vortex depth, 1000 cP.

4.5 1000 cP Trends

The Pareto significant factors for the 1000 cP are shown in Table 8, and the model and main effects plot can be found in Appendix F. From the Pareto analysis, the only statistically significant parameter is Fr, with increasing Fr causing an increase in the maximum vortex depth. This suggests that, while other parameters may play a role, in our data Fr overshadows their effects. This means that to produce the desired maximum vortex depth, Fr should be monitored carefully, while other parameters can take a range of values. The R^2 value for the model is 0.3945, with a well-ranked model F-value of 18.90.

4.6 Discussion

In analyzing the main effect of parameters, maximum vortex depth was expected to increase with increasing tank size because the whole system scales up. While this is the trend for all scenarios and is a statistically signficant factor for 1 cP, tank size is not statistically significant for the other viscosities or for all of the data combined. This can be explained by the fact that in the higher viscosity systems, other parameters such as Fr simply have a larger effect and overshadow the impact of tank size. This suggests that maximum vortex depth is a weaker function of the other parameters for this viscosity. It is suspected, then, that viscosity plays a magnifying role on the effect of other parameters, something which should be noted when trying to build a correlation.

While analyzing all of the data collected, it was determined that the normality of the residuals for each model was normal (see Appendices B-F). Models created to include all of the factors yielded R^2 values ranging from 0.70 to 0.88, which shows that the data was relatively consistent. However, when the models were normalized to include only statistically significant factors, the model R^2 values decreased to 0.16 to

0.6042. The 100 cP model best fits the data. This is because the 100 cP material formed more stable vortices that were easier to characterize than the 1 cP material, and which produced results for most all of the trials done (unlike the 1000 cP material). The low R^2 values are due to insufficient collected data, and could also be influenced by the fact that Fr was intentionally changed between each trial. Consistently, the Fr number held one of the the lowest p-values and the highest F-value for each model, meaning that, as was expected, the Fr number is one of the most significant parameters in maximum vortex formation. The exception to this is the average vortex depth dataset, which indicates that the stability and steady state formation of vortices is a more complex phenomena that depends on the interaction of multiple factors.

An analysis for stability was inconclusive, showing no statistically significant factors, as can be seen in Appendix G. The meaning behind this is twofold: first, it indicates that vortex stability is a complex characteristic that depends on a number of two and three way factor interactions. Second, vortex stability is a difficult characteristic to quantify, so there could be several errors with the method with which stability was quantified.

5 Future Work

In analyzing data, vortex stability was considered by tracking the fraction of time in each trial that a vortex was present. However, this form of analysis fails to take into account the depth reached at this time, and many systems can display multiple stable heights, or an oscillating vortex. This complexity is most relevant for the 1 and 100 cP trials, which would be of more interest in an industry setting.

In the future, we recommend that more trials be done over a wider range of Fr numbers to stabilize the models, especially for 1000 cP trials, some of which did not generate vortices. Specifically, no vortex formation occurred for the conditions listed in Table 9. The R^2 values for each of the models are relatively low, so more data would improve these models as well. It is also recommended that in analyzing the vortex trials, time weighted averages be taken for the appearance of the vortex in order to characterize vortex stability.

6 Conclusion

The goal of this project was to explore vortex formation in a partially-baffled tank. This is particularly of interest to companies like SPX when it comes to solid incorporation in mixing, and industries like wastewater treatment and fermentation require some sort of vortex to fully mix solids into the solution. Experiments examined the development of vortices in a partially baffled system because the partial baffles allow for sufficient shearing forces to mix the fluid, while allowing vortex formation above the baffles. The parameters explored include coverage, impeller diameters, mixing speeds, tank size, and material viscosity. A factorial design of experiment was implemented to analyze these parameters. A factorial regression was used to create a model for maximum vortex depth for 1 cP, 100 cP, 1000 cP, and all of the data together. A model and effect plot was also created to predict average vortex depth for the viscosity trials that showed stable vortices.

Partially baffled systems are complex systems to model, and hopefully the data gathered in this project provides the mixing industry with more insight into vortex predictions for partially-baffled tanks.

Tank	Viscosity	Impeller Diameter	Coverage
11.5"	100 cP	2.3"	1
11.5"	1000 cP	2.3", 3.36"	.67, 1
17.5"	1000 cP	5.08"	.33, .67, 1

Table 9: Conditions for which no vortex formed.

7 Special Thanks

We would like to thank Professor David Foster for being our faculty advisor and giving insightful consultation and Thor Olsen for providing the LabView code for the mixing tank. We would also like to thank our contacts at SPX, Kevin Logsdon, Aaron Strand, and Richard Kehn, for sponsoring the investigation and providing all the necessary equipment. Lastly we would like to thank our teaching assistant, Wenshi Zhang, for providing her assistance in the logistics of the project.

References

[1] Sara Peters. Baffled by baffle size for industrial mixing. blog.craneengineering.net/baffled-by-baffle-size-for-industrial-mixing, November 2016. Accessed: 2 October 2018.

[2] Kar K.K. et al. Deshpande, S.S. An experimental and computational investigation of vortex formation in an unbaffled stirred tank. *Chemical Engineering Science*, 168:495–506, 2017.

8 Appendices

A: Parameter Letter Assignments

Parameter	Label
μ	A
T	B
D/T	C
COV/D	D
Fr	E

B: Average Vortex Depth, All Data

$$\Delta_{avg}(in) = 0.7619 + 0.343CD$$

R^2: 11.20%, Model F-value: 9.59

Parameter	F Value
CD	9.59

Parameter	Significance
CD	$p < 0.01$

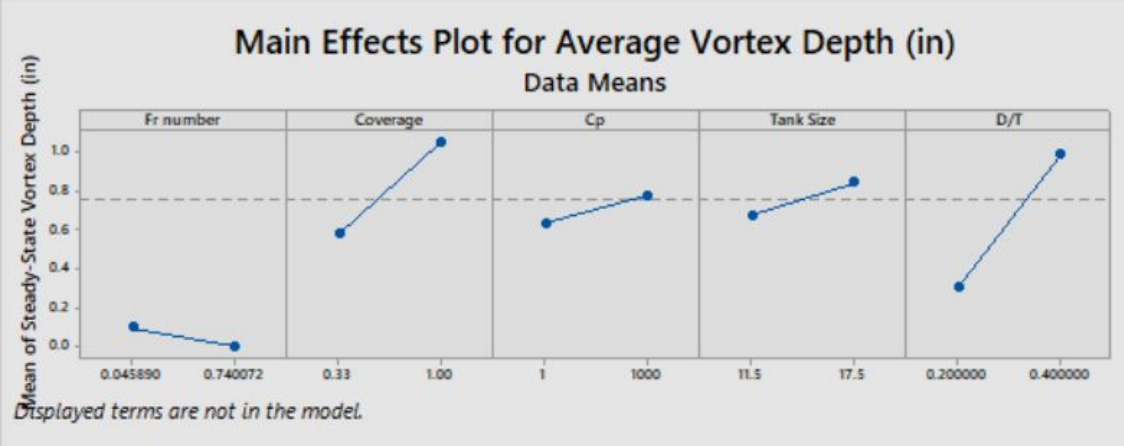

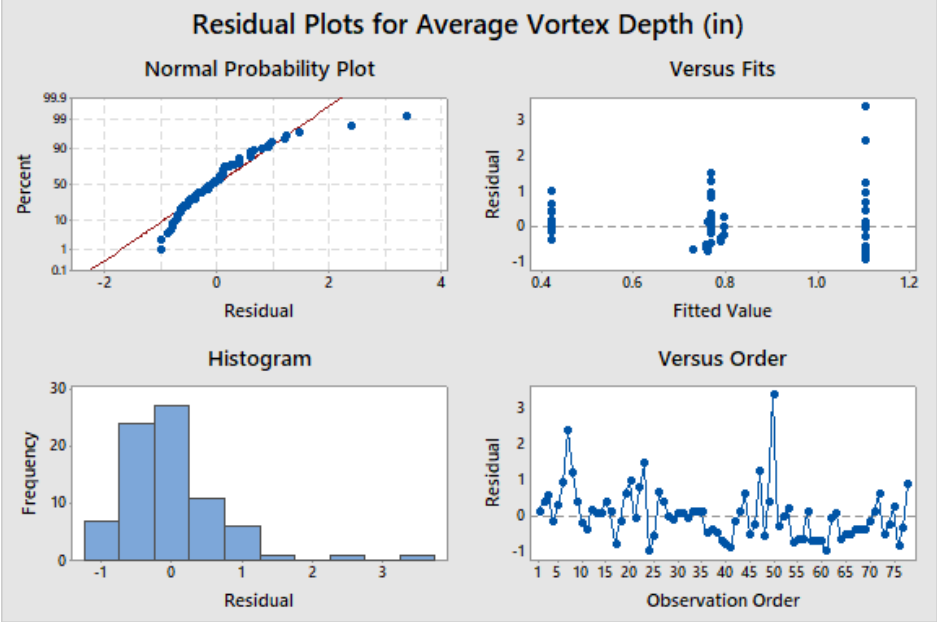

C: Maximum Vortex Depth, All Data

$\Delta_{max}(in) = -0.130 + 3.859E + 2.80C$

R^2: 33.19%, Model F-value: 33.28

Parameter	F Value
E	60.78
C	5.08

Parameter	Significance
E	$p < 0.01$
C	$p < 0.05$

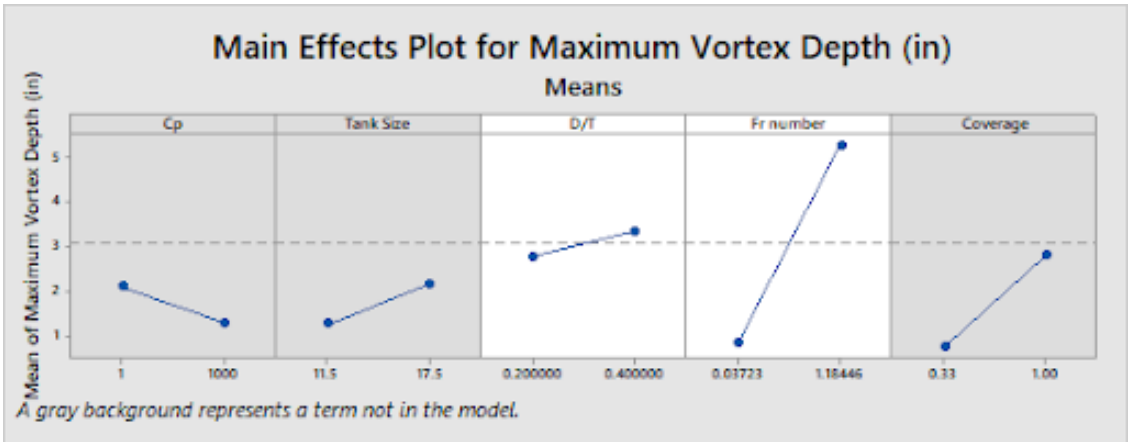

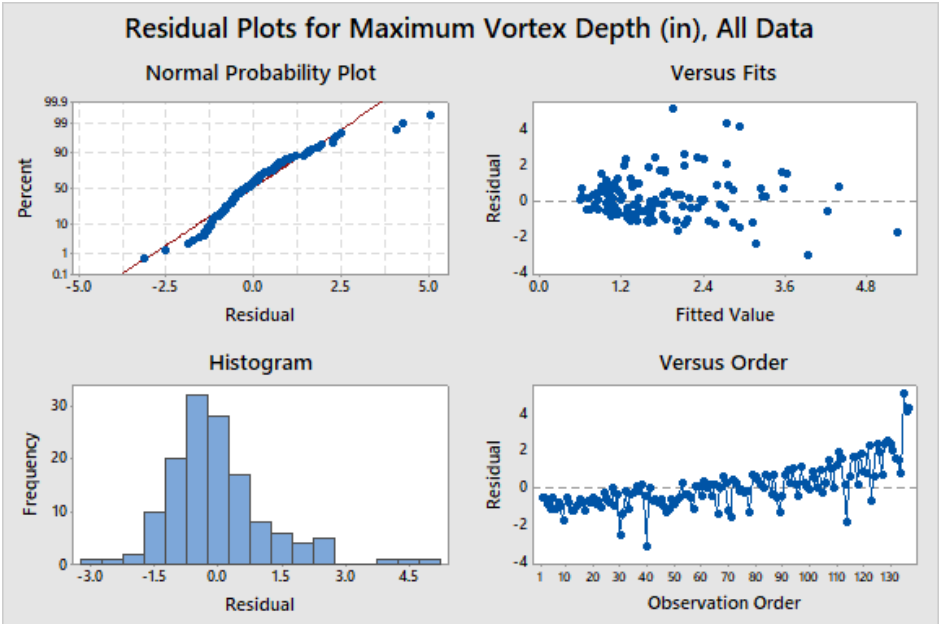

D: Maximum Vortex Depth, 1 cP

$$\Delta_{max}(in) = -2.303 + 0.1522B + 4.00C + 4.293E$$

R^2: 47.67%, Model F-value: 15.49

Parameter	F Value
E	36.83
B	9.49
C	4.80

Parameter	Significance
E	$p < 0.01$
B	$p < 0.01$
C	$p < 0.05$

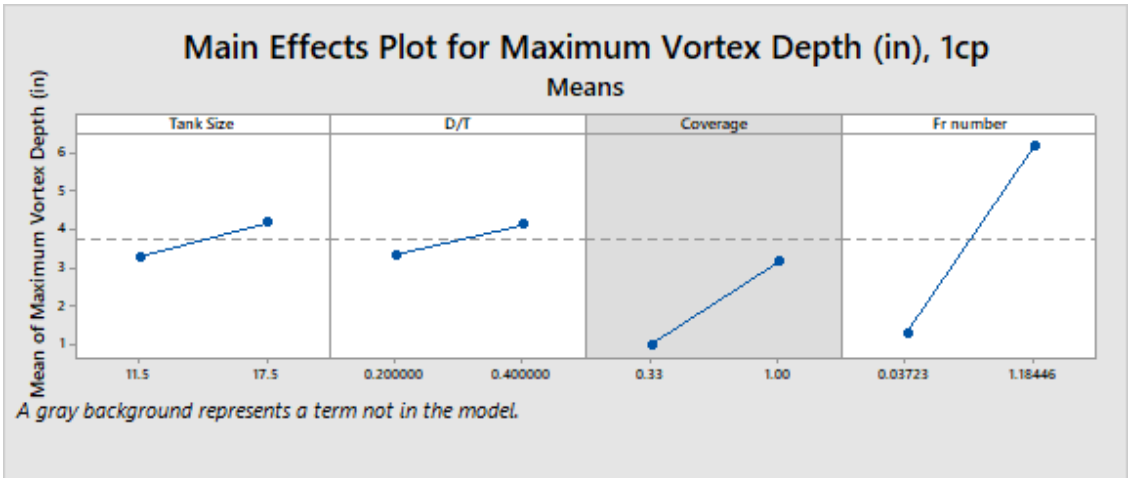

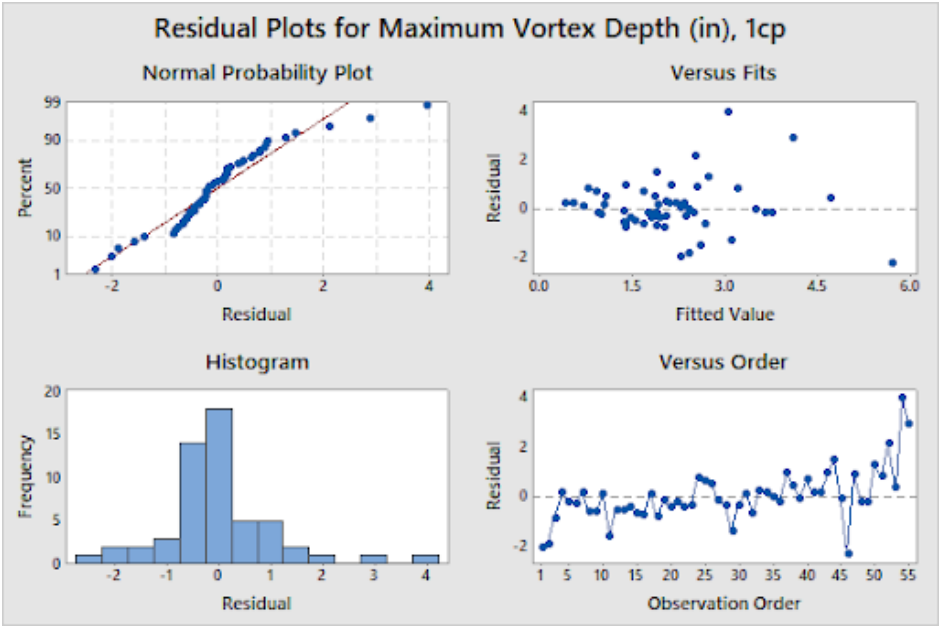

E: Maximum Vortex Depth, 100 cP

$$\Delta_{max}(in) = 3.147 + 2.606E + 2.469CD + 2.849CDE$$

R^2: 60.42%, Model F-value: 23.92

Parameter	F Value
E	57.31
CD	11.74
CDE	9.53

Parameter	Significance
E	$p < 0.01$
CD	$p < 0.01$
CDE	$p < 0.01$

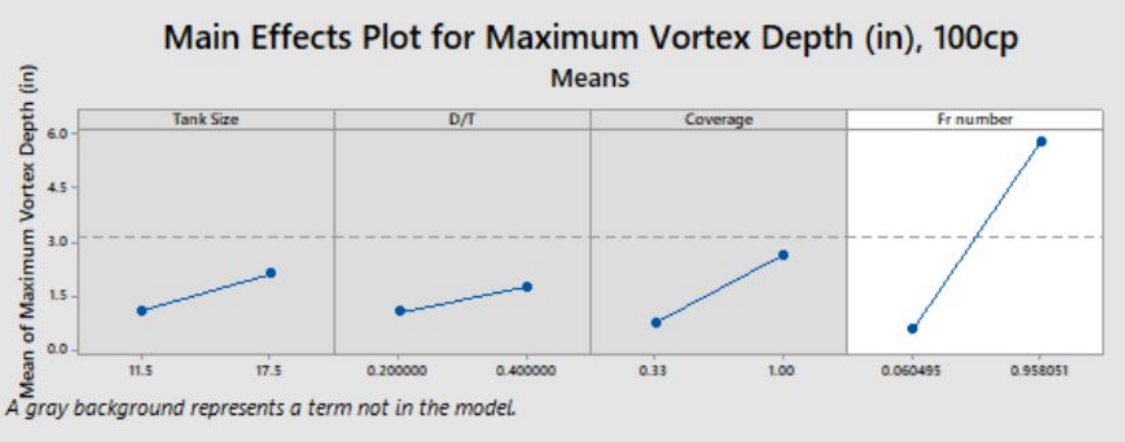

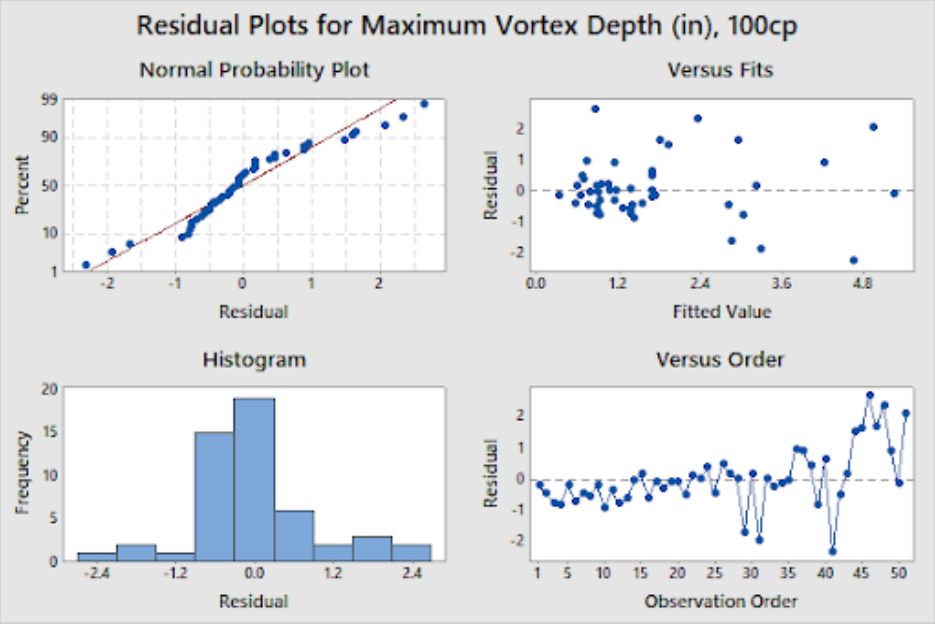

F: Maximum Vortex Depth, 1000 cP

$$\Delta_{max}(in) = 0.041 + 3.517E$$

R^2: 39.45%, Model F-value: 18.90

Parameter	F Value
E	18.90

Parameter	Significance
E	$p < 0.01$

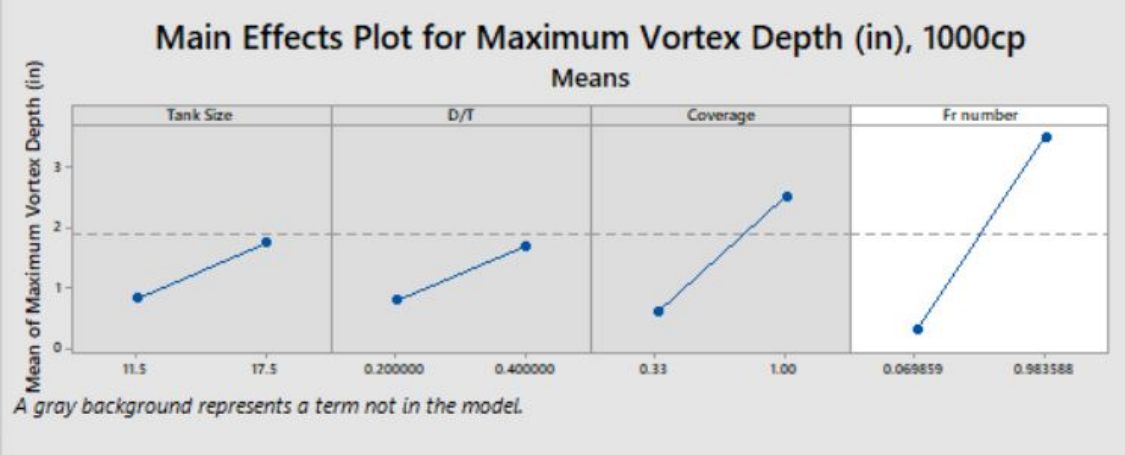

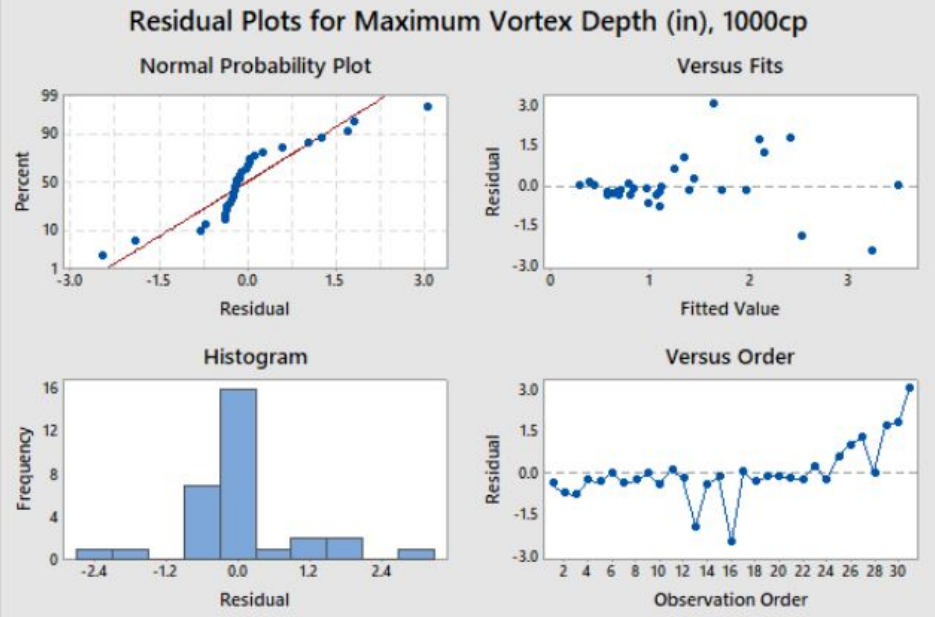

G: Pareto Plots for 32 Parameter Fits

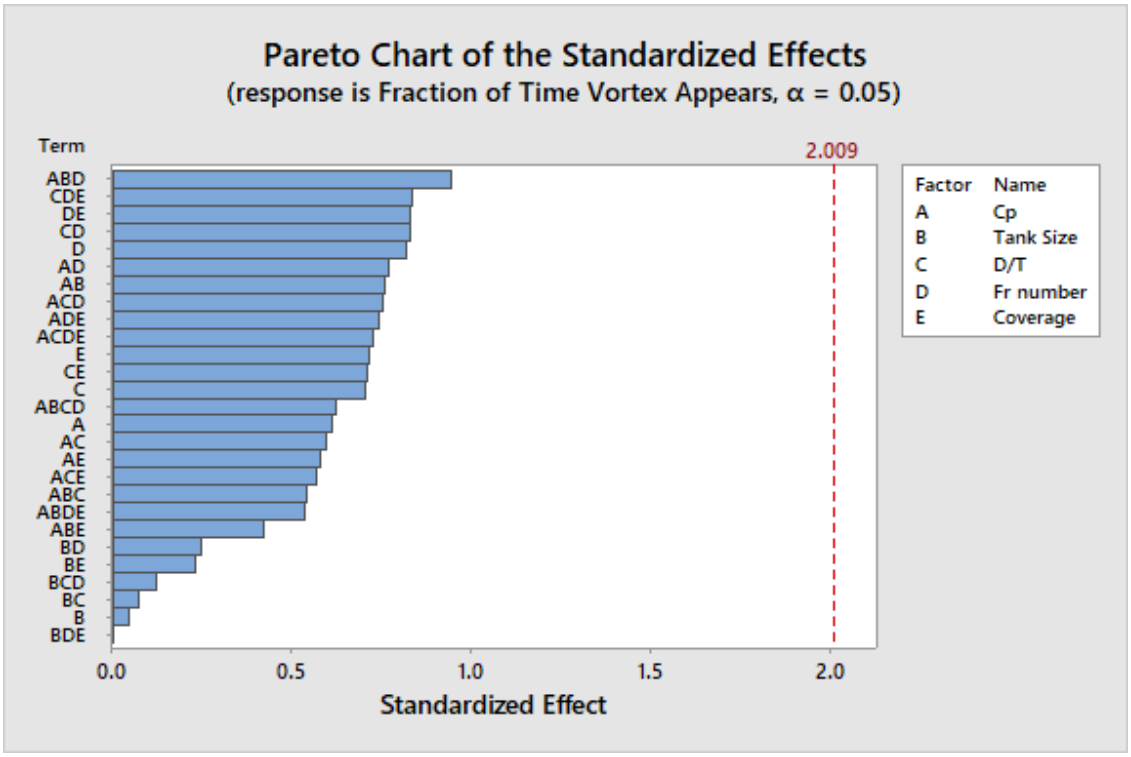

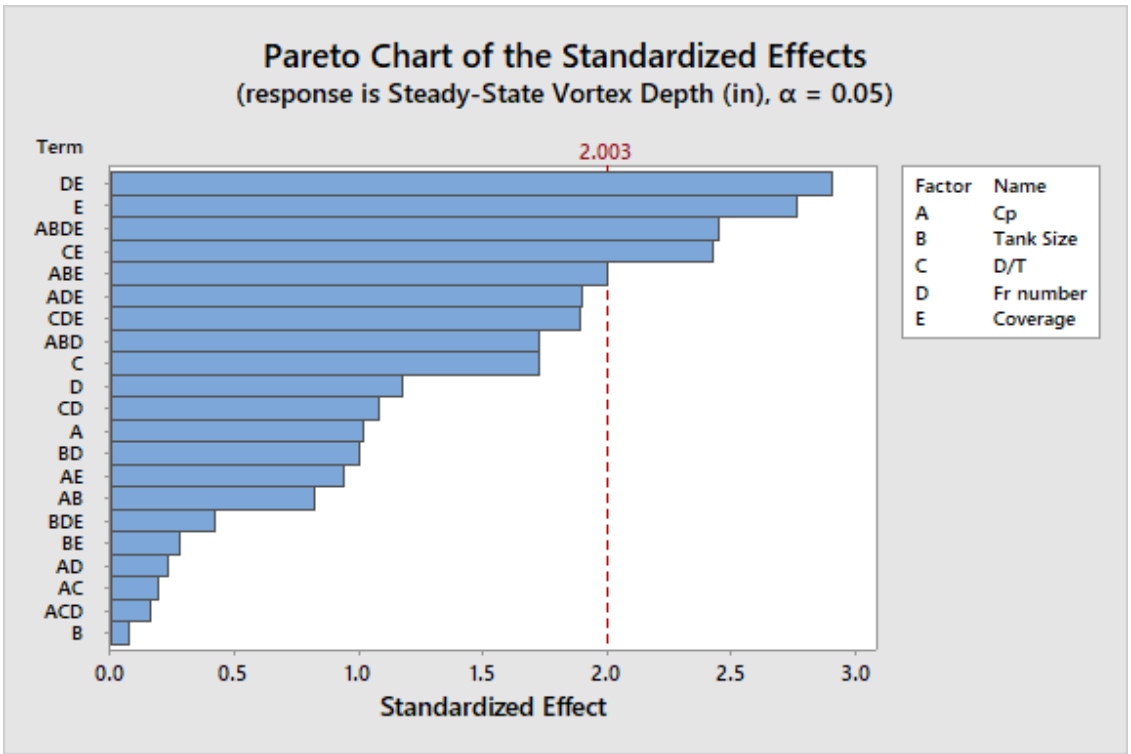

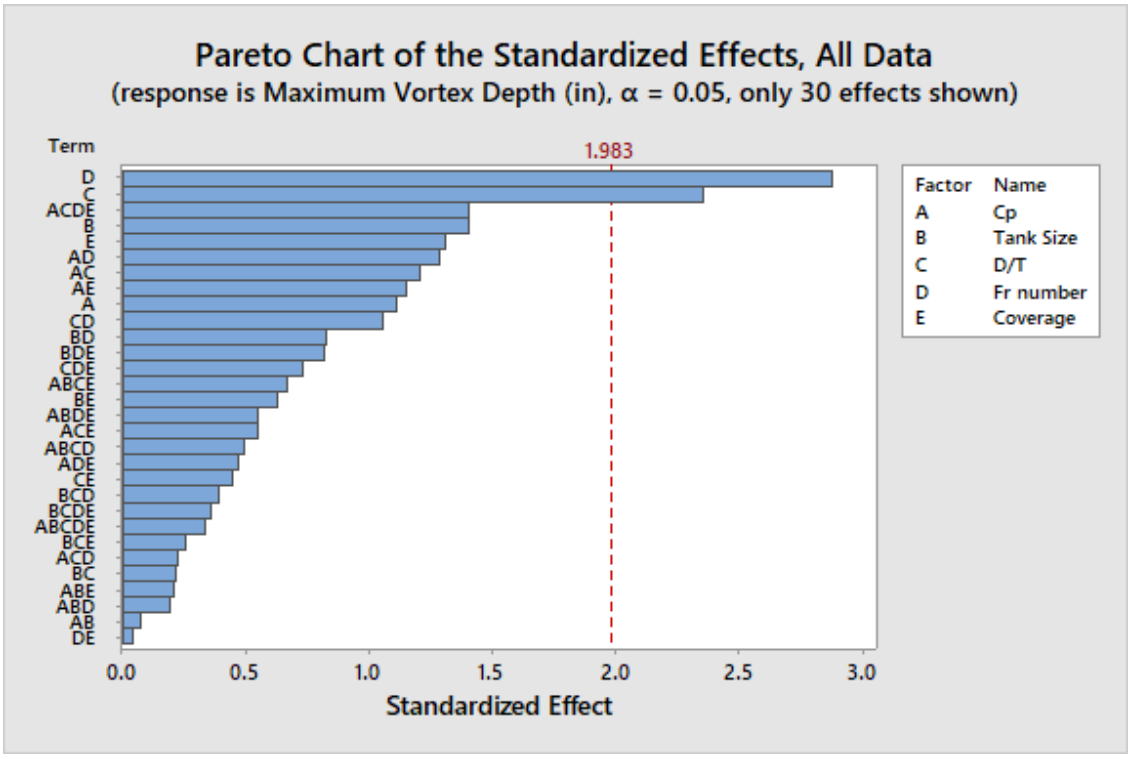
Pareto Chart of the Standardized Effects, All Data
(response is Maximum Vortex Depth (in), α = 0.05, only 30 effects shown)
Term
1.983
D
C
ACDE
B
E
AD
AC
AE
A
CD
BD
BDE
CDE
ABCE
BE
ABDE
ACE
ABCD
ADE
CE
BCD
BCDE
ABCDE
BCE
ACD
BC
ABE
ABD
AB
DE
0.0
0.5
1.0
1.5
2.0
2.5
3.0
Standardized Effect
Factor Name
A Cp
B Tank Size
C D/T
D Fr number
E Coverage

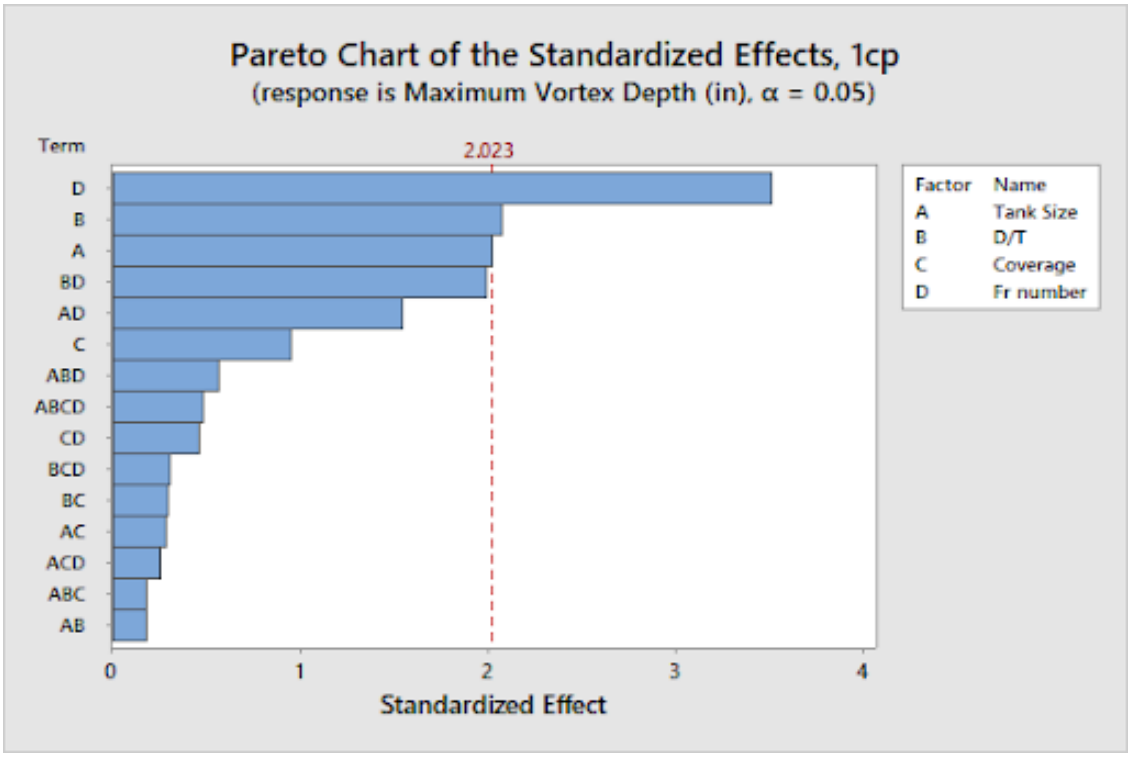
Pareto Chart of the Standardized Effects, 1cp
(response is Maximum Vortex Depth (in), α = 0.05)
Term
2.023
D
B
A
BD
AD
C
ABD
ABCD
CD
BCD
BC
AC
ACD
ABC
AB
0
1
2
3
4
Standardized Effect
Factor Name
A Tank Size
B D/T
C Coverage
D Fr number

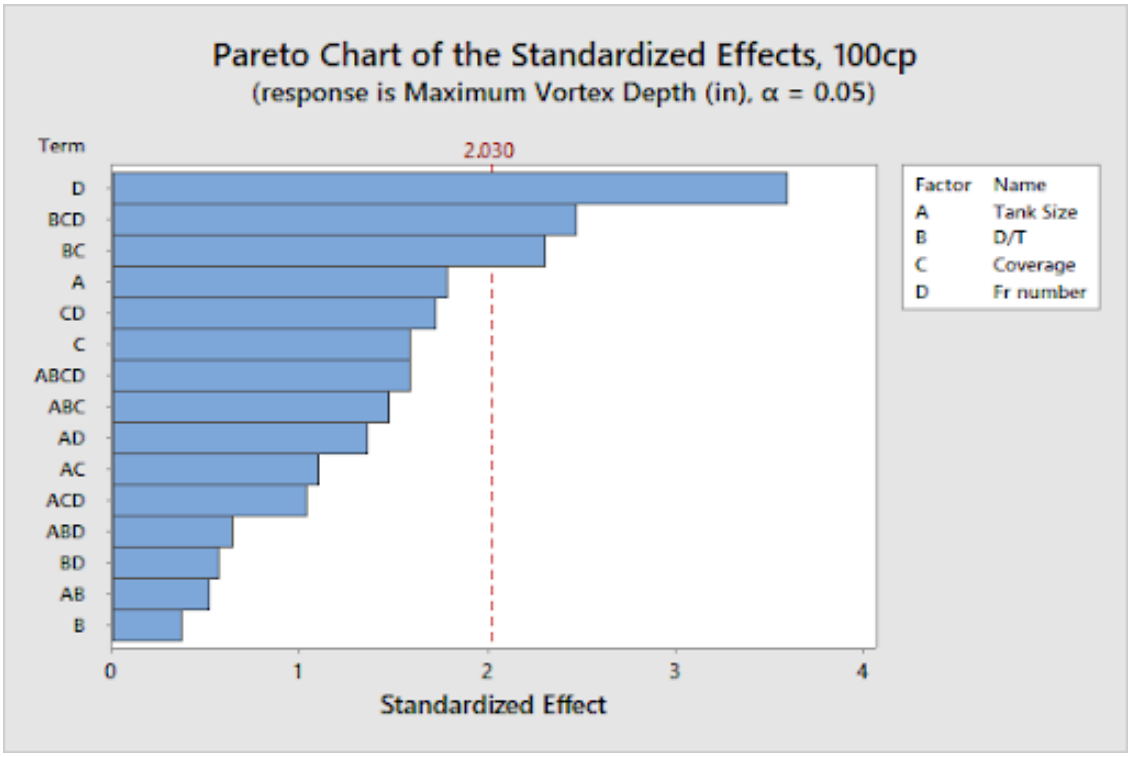
Pareto Chart of the Standardized Effects, 100cp
(response is Maximum Vortex Depth (in), α = 0.05)
Term
2.030
D
BCD
BC
A
CD
C
ABCD
ABC
AD
AC
ACD
ABD
BD
AB
B
0
1
2
3
4
Standardized Effect
Factor Name
A Tank Size
B D/T
C Coverage
D Fr number

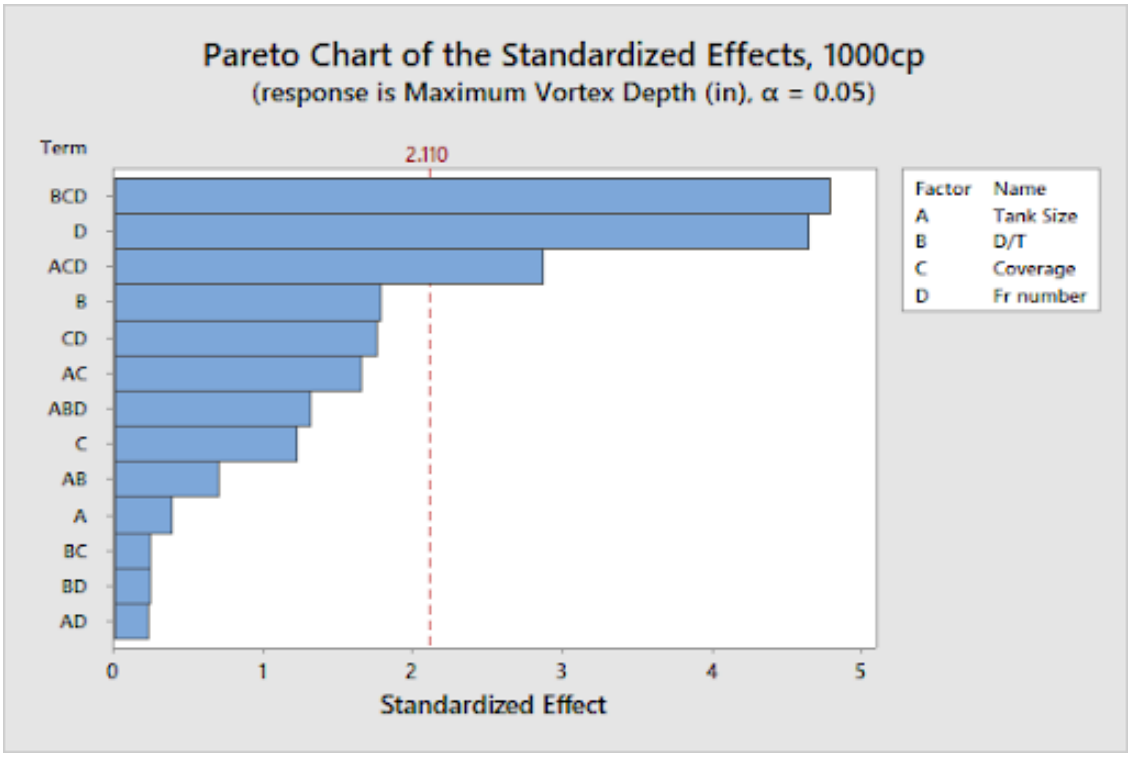
Pareto Chart of the Standardized Effects, 1000cp
(response is Maximum Vortex Depth (in), α = 0.05)
Term
2.110
BCD
D
ACD
B
CD
AC
ABD
C
AB
A
BC
BD
AD
0
1
2
3
4
5
Standardized Effect
Factor Name
A Tank Size
B D/T
C Coverage
D Fr number

H: P&ID